Modeling Spectral LED Degradation Using an Unsupervised Machine Learning Approach

Herzog, Alexander; Hamon, Benoit; Myland, Paul; Foerster, Peter; Benkner, Simon; Zandi, Babak; Guerra, Victor; Schoeps, Sebastian; Van Driel, Willem D.; Khanh, Tran Quoc

DOI
10.1109/ACCESS.2025.3592806

Publication date
2025

Document Version
Final published version

Published in
IEEE Access

IEEE Access
Multidisciplinary | Rapid Review | Open Access Journal

Received 3 July 2025, accepted 23 July 2025, date of publication 25 July 2025, date of current version 31 July 2025.

Digital Object Identifier 10.1109/ACCESS.2025.3592806

RESEARCH ARTICLE

Modeling Spectral LED Degradation Using an Unsupervised Machine Learning Approach

ALEXANDER HERZOG[1], (Senior Member, IEEE), BENOIT HAMON[2], PAUL MYLAND[1], PETER FOERSTER[3], (Senior Member, IEEE), SIMON BENKNER[1,4], BABAK ZANDI[1], VICTOR GUERRA[2], SEBASTIAN SCHOEPS[3], (Senior Member, IEEE), WILLEM D. VAN DRIEL[5,6], AND TRAN QUOC KHANH[1]

[1]Laboratory of Adaptive Lighting Systems and Visual Processing, Technische Universität Darmstadt, 64289 Darmstadt, Germany
[2]PI Lighting, 1950 Sion, Switzerland
[3]Computational Electromagnetics Group, Technische Universität Darmstadt, 64289 Darmstadt, Germany
[4]klion GmbH, 64295 Darmstadt, Germany
[5]Electronic Components, Technology and Materials (ECTM), Department of Microelectronics, Delft University of Technology, 2628 CD Delft, The Netherlands
[6]Signify, 5656 AE Eindhoven, The Netherlands

Corresponding author: Alexander Herzog (herzog@lichttechnik.tu-darmstadt.de)

This work was supported by the Electronics Components and Systems for European Leadership (ECSEL) Joint Undertaking (JU), funded by European Union's Horizon 2020 Research and Innovation Program and The Netherlands, Hungary, France, Poland, Austria, Germany, Italy, and Switzerland, under Grant 101007319.

ABSTRACT The modeling of spectral characteristics of light-emitting diodes (LED) has been addressed in various studies. We extend the current state of knowledge by modeling the spectral characteristics of commercially available high-power LEDs, exhibiting a temperature-dependent degradation, by using a different modeling strategy. To this end, the state of the art approach of an additive superposition of probability density functions (PDF) is compared with an unsupervised machine learning approach called non-negative matrix factorization (NMF). The stress test data used in our modeling routine was collected for a period of 6000 hours at four different case temperatures between 55 °C and 120 °C. The results of the accelerated stress tests indicate a temperature-activated aging process, which can be described using the Arrhenius equation. By combining the Arrhenius equation with the modeling parameters, the spectral characteristics can be modeled for 6000 hours of stress at four different stress test temperatures. The introduced spectral modeling approach using non-negative matrix factorization achieves CIE 1976 UCS chromaticity differences primarily smaller than $\Delta u'v' \leq 0.001$ and proves to be superior to superimposed probability density functions in terms of colorimetric reconstruction accuracy, modeling complexity and robustness against spectral outliers.

INDEX TERMS Light-emitting-diodes (LED), power distribution, non-negative matrix factorization, spectral modeling, LED reliability, digital twin, spectral analysis.

I. INTRODUCTION

Over the past decades, the use of LEDs as a compact energy-saving light source has become established in various applications. To ensure reliable operation of the devices, their lifetime and the associated dependence on operating conditions has been addressed in numerous studies [1], [2], [3], [4]. Thus, several approaches for lifetime modeling and the associated radiant flux depreciation have become standardized, allowing to approximate, model and extrapolate the radiant flux in dependence of operating time, temperature and current [5]. Nevertheless, these modeling approaches do not consider the spectral information, although it is essential for the calculation of various visual and non-visual metrics [6], [7], [8], [9], [10], [11]. In contrast to radiant flux decay modeling, the modeling of spectral characteristics is much more complex, both in steady state and for the operating time [12], [13], [14]. Spectral steady state characteristics, which exclude effects of device degradation, are affected by operating temperature and forward current [15]. The emitter

The associate editor coordinating the review of this manuscript and approving it for publication was Jiajie Fan.

junction temperature and thus the emitted spectrum directly depends on the case temperature and the applied forward current due to Joule heating effects. Variations of these operating parameters result in spectral shifts of the emission spectrum and in variations of the total emitted radiant flux.

Furthermore, the spectral characteristics for times beyond the steady state condition are also driven by various parameters. The operating current, temperature and prevailing humidity directly accelerate the degradation mechanisms of the device [16], [17], [18], [19], [20], [21]. Multiple degradation processes in the die or package of the device are impacting the emission of the LED's active region (AR) or its transmission through the device's package [18]. As a result, the spectral properties of light-emitting diodes tend to change during their lifetime [16], [19], [20], [22], [23], [24].

Current approaches, modeling the spectral characteristics of quasi-monochromatic and phosphor-converted LEDs by an additive superposition of probability density functions (PDF), can exhibit significant colorimetric deviations depending on the type and number of the selected density functions [15], [25], [26], [27], [28], [29], [30], [31], [32], [33], [34], [35], [36], [37], [38]. Depending on the complexity of the spectral characteristics, a higher number of superimposed probability density functions is required to ensure colorimetrically imperceptible deviations from the original spectrum [39]. Recent findings suggest that flexible alternatives, such as split Pearson-VII functions, can provide significantly improved spectral reconstructions compared to Gaussian mixtures at the same model complexity [39]. These enhanced fit functions are capable of modeling asymmetric peak shapes and reduce colorimetric errors, which is particularly beneficial for phosphor-converted white LEDs. However, they still reach their limitations when it comes to accurately representing the sharp and narrow-band emission characteristics of KSF phosphors [40], [41].

In the case of spectral modeling over lifetime or for different operating parameters, a large number of independent variables has to be modeled, significantly affecting the spectral reconstruction error [39]. Furthermore, in some cases the parameters can hardly be interpolated using established models, additionally increasing the complexity of the approach [39].

The original contribution of this paper is the introduction of a different spectral modeling approach that combines an existing physics-based model for temperature-dependent radiant flux depreciation with an unsupervised machine learning approach. In order to assess the added value of non-negative matrix factorization compared to the commonly used superposition of probability density functions, both approaches are evaluated and compared on a uniform and representative spectral degradation data set.

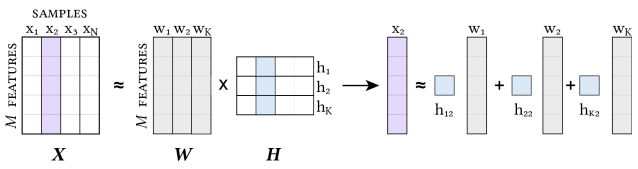

FIGURE 1. Schematic NMF decomposition of a non-negative matrix **X** [44].

II. EXPERIMENTAL DETAILS

A. SAMPLES

The spectral modeling is performed on aging data of commercially available 175 W high-power Chip-on-Board (COB) modules with a correlated color temperature (CCT) of 4500 K and a color rendering index (CRI) of 80. The stress tests have been carried out for a period of 6000 hours at four different case temperatures ($T_c = 55, 85, 105, 120\,°C$) with four LEDs each and a constant stress current of $I_a = 3300\,mA$. The LED spectra were measured in intervals of 1000 hours using a 1 m-integrating sphere with 2π-geometry and a spectroradiometer (CAS140CT - Instrument Systems). Thus, a total number of 112 spectra were measured. Since this paper only addresses the spectral degradation modeling, a detailed analysis of the device structure, experimental setup and underlying degradation mechanisms can be found in a recent published work by Herzog et al. [42]. Therefore, only relevant information for spectral modeling will be reported within the results section.

B. CONCEPT OF NON-NEGATIVE MATRIX FACTORIZATION

Non-negative matrix factorization (NMF) is an unsupervised machine learning technique used to approximate non-negative data matrices by a low-rank decomposition. The input matrix $\mathbf{X} \in \mathbb{R}_{\geq 0}^{M \times N}$, containing N non-negative observation vectors $\mathbf{x}_1, \ldots, \mathbf{x}_N \in \mathbb{R}_{\geq 0}^{M}$, is factorized into two lower-dimensional matrices $\mathbf{W} \in \mathbb{R}_{\geq 0}^{M \times K}$ and $\mathbf{H} \in \mathbb{R}_{\geq 0}^{K \times N}$, such that $\mathbf{X} \approx \mathbf{WH}$ [43], [44].

Each observation $\mathbf{x}_n$ is thus represented as a linear combination of K basis spectra $\mathbf{w}_k$, with corresponding non-negative coefficients h_{kn}. A schematic of the decomposition is shown in Fig. 1.

One major advantage of NMF in the context of spectral modeling is the non-negativity constraint, which ensures that the extracted basis vectors $\mathbf{w}_k$ can be directly interpreted as physically meaningful spectral components. This makes NMF particularly suitable for analyzing and reconstructing emission spectra of LEDs, where negative values are physically implausible.

The decomposition is typically formulated as an optimization problem that minimizes the distance between the input matrix $\mathbf{X}$ and its approximation $\mathbf{WH}$. In this work, the squared Frobenius norm is used as the cost function:

$$\min_{\mathbf{W},\mathbf{H} \geq 0} \|\mathbf{X} - \mathbf{WH}\|_F^2 = \sum_{i=1}^{M} \sum_{j=1}^{N} \left(X_{ij} - (WH)_{ij}\right)^2 . \quad (1)$$

This objective encourages a reconstruction that minimizes the total squared error across all spectral samples. The optimization is performed using iterative multiplicative

update rules, which maintain non-negativity throughout the process.

The decomposition was implemented using the Scikit-learn 1.2.0 library [45]. The measured absolute spectra were used directly as input vectors without preprocessing or normalization. Spectra measured at $t = 0\,\text{h}$ and $t = 6000\,\text{h}$ were provided as initial guesses for the basis vectors $\mathbf{w}_k$, enabling a physically informed initialization.

C. CONCEPT OF SUPERIMPOSED PDFS

As an alternative to NMF, the spectral power distribution of LEDs can also be decomposed into a sum of constituent functions, which represents the most commonly used approach for spectral modeling. The quantity and the nature of the superimposed functions heavily depends on the complexity of the LED spectrum. In this paper, a decomposition into individual Gaussians has been performed on the measured spectra, by using the Gaussian probability density function

$$f(\lambda\,|\,p_1, p_2, p_3) = p_1 \cdot \exp\left(-\left(\frac{(\lambda - p_2)}{p_3}\right)^2\right) \quad , \qquad (2)$$

with wavelength λ and three parameters p_1, p_2 and p_3. An example of two superimposed Gaussians g_1 and g_2 is shown in Figure 2. As a starting point for the Gaussian decomposition, two Gaussians have been considered to represent the blue emitters excitation peak and one Gaussian per phosphor type used in the phosphor converted part of the spectrum. From this baseline, the number of Gaussians has been adjusted to optimize the balance between the goodness of fit and the number of parameters. The optimum of the number of Gaussians is identified automatically by analyzing the evolution of both coefficient of determination and root mean square error. To enhance the consistency of the model parameters, the spectra are normalized to a reference optical power of 1 W, thereby focusing the model on the spectral shape. The full spectral profile can then be reconstructed by scaling the normalized shape with the actual optical power.

To define a reference set of model parameters, all measured spectra from pristine samples were summed and normalized. The model parameters were obtained by using a dedicated algorithm that automatically identifies the positions of the chip and phosphor emission peaks and subsequently finds the optimized number of Gaussians. The obtained parameter set is used as a solver starting point to model the aged spectra, thus allowing the generation of consistent model parameters gradually evolving with increasing stress time.

Both approaches were evaluated by calculating commonly used radiometric and photometric metrics for LED spectral modeling [39], including the relative difference in radiant flux ΔP_{opt}

$$\Delta P_{\text{opt}} = (P_{\text{opt,NMF}}/P_{\text{opt,true}} - 1) \cdot 100\,\% \qquad (3)$$

and the Euclidean chromaticity difference $\Delta u'v'$:

$$\Delta u'v' = \sqrt{(u'_{\text{NMF}} - u'_{\text{true}})^2 + (v'_{\text{NMF}} - v'_{\text{true}})^2} \qquad (4)$$

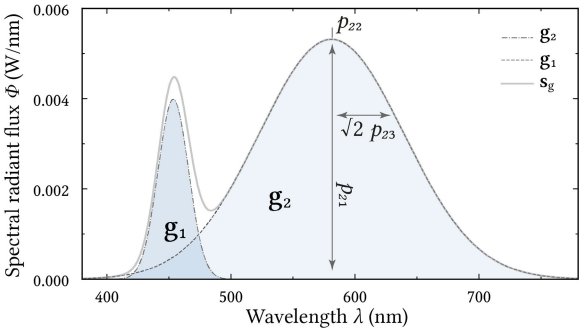

FIGURE 2. Schematic illustration of the approximated spectrum s_g by two superimposed Gaussian probability density function g_1 and g_2.

Since it is not possible to assign the explained variance (EV) to each particular NMF component, the total explained variance is determined.

III. RESULTS

A. DEGRADATION TEST

The results obtained from the conducted degradation test reflect typical temperature-dependent degradation behavior observed in white LEDs and thus provide representative data for this study. Fig. 3 (a) shows the radiant flux depreciation for different case temperatures and an aging current of $I_a = 3300\,\text{mA}$.

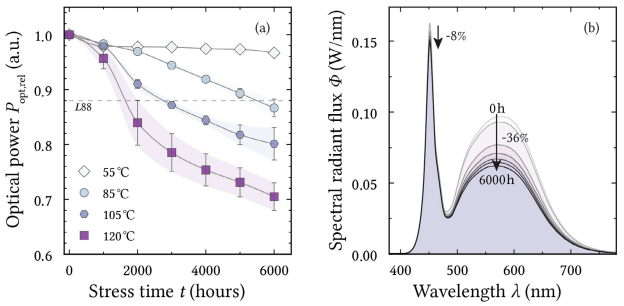

FIGURE 3. (a) Decrease in relative radiant flux $P_{\text{opt,rel}}$ for a period of 6000 hours at four different case temperatures. The reported values represent the arithmetic mean with its respective standard deviation. (b) Spectral characteristics for 6000 hours of stress testing at a case temperature of $T_c = 105\,°\text{C}$.

Within 6000 hours of stress, an optical power loss of up to 30 % can be observed, indicating a strong temperature dependence. Depending on junction temperature, there is an exponential decrease in time to failure, that could be described using the reciprocal Arrhenius equation. The occurrence of the mean time to failure criterion ($MTTF$) as a function of junction temperature T_j is obtained using

$$MTTF(T_j) = C \cdot \exp\left[\frac{E_a}{k_B T_j}\right] \qquad (5)$$

with activation energy E_a, Boltzmann constant k_B and coefficient C. Fitting the logarithmic L_{88}-lifetimes vs. inverse junction temperatures manifests the temperature-accelerated

aging process, which can be described with a coefficient of determination of $R^2 = 0.99$ using the Arrhenius equation, shown in Fig. 4. The derived activation energy can be quantified with $E_a = 0.43$ eV, thus allowing to interpolate and model the *MTTF* for the defined radiant flux failure criterion at various temperatures. The gradual radiant flux depreciation

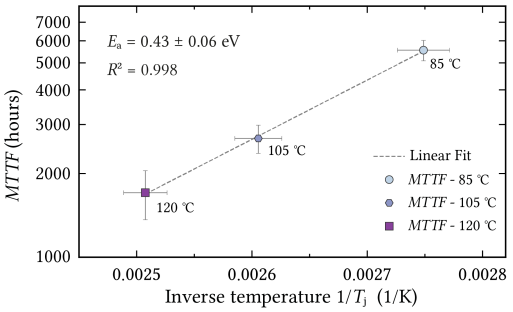

FIGURE 4. Mean time to failure vs. inverse junction temperatures at a failure criterion defined at 88 % of the initial radiant flux. The derived activation energy can be quantified with $E_a = 0.43$ eV.

is accompanied by an imbalanced reduction of spectral components, shown representatively for a temperature of $T_c = 105\,°C$ in Fig. 3 (b). These spectral imbalances result in a visually perceptible color shift of the chromaticity coordinates, shifting almost linearly in the CIE 1976 UCS with increasing stress time, see Fig. 7 (b). In addition, the Euclidean chromaticity distance with respect to the initial spectrum $\Delta u'v'$, correlates linearly with the decrease in radiant flux (not shown here). Consequently, it is possible to infer the optical degradation from the color shift and vice versa.

B. NON-NEGATIVE MATRIX FACTORIZATION

The observation matrix $\boldsymbol{X}$, containing all spectra measured throughout the aging period under various aging conditions (a total of 112 spectra), is approximated with different numbers of components, $K \in 1, 2, 3, 4$. As a result, the NMF extracts K basis spectra with K weights per observation, allowing to reconstruct the initial observation matrix. Table 1 shows the evaluation results for the different numbers of components. With an increasing number of components, the error in the considered metrics decreases, while the total explained variance (EV) improves. There is a significant error reduction between one and two components, which is only slightly reduced for $K \geq 3$.

TABLE 1. Evaluation of NMF solutions for four different numbers of components with averaged values for relative difference in radiant flux and chromaticity difference.

K	$\Delta u'v'$	$\lvert \Delta P_{\mathrm{opt,rel}} \rvert$ (%)	EV (%)
1	0.00581	0.530	60.6
2	0.00039	0.090	86.7
3	0.00039	0.097	94.5
4	0.00029	0.025	96.0

In addition, when using more than two components, the required linear or at least smooth and continuous correlation between radiant flux depreciation and the factorization weights is no longer observed. This correlation is essential to enable the integration of physics-based models, such as those describing the temperature dependence of the optical power based on the Arrhenius equation, with the non-negative matrix factorization approach. As a consequence, a factorization with two components proves to be target-oriented for the problem considered, being described in detail below. A schematic overview of the procedure for combining the temperature- and time-dependent radiant flux model with the spectral non-negative matrix factorization approach is presented in Fig. 5.

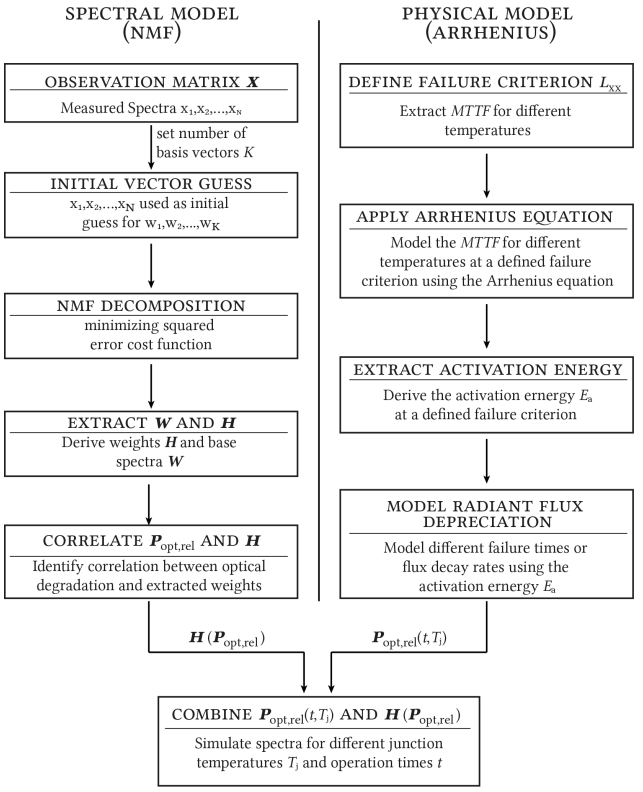

FIGURE 5. Schematic overview of the procedure for combining the temperature- and time-dependent radiant flux model with the spectral non-negative matrix factorization approach. The figure illustrates how the physics-based modeling of radiant flux depreciation, described by the Arrhenius equation, is linked with the factorization weights obtained from NMF to enable temperature-dependent spectral modeling over time.

The extracted basis vectors for $K = 2$ are shown in Fig. 6 (a), whereas Fig. 6 (b) shows the corresponding chromaticity coordinates in CIE 1976 UCS. Fig. 7 (a) shows the determined weights (h_{1n}, h_{2n}) plotted against the relative optical power loss, revealing a distinct linear correlation. This relationship enables the modeling of the weight coefficients as a function of the relative radiant flux depreciation and its temperature dependence, as described by a physics-based model based on the Arrhenius equation. This allows to reconstruct the spectra for different values of relative radiant

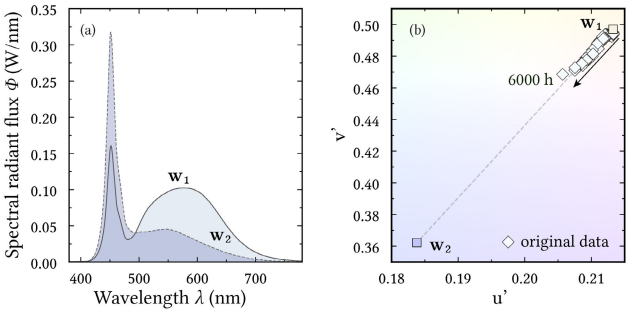

FIGURE 6. (a) Basis vectors w_1 and w_2 of NMF decomposition with two components $K = 2$. (b) CIE 1976 UCS with original data and corresponding chromaticity coordinates for w_1 and w_2.

flux and thus for various aging conditions and operation times.

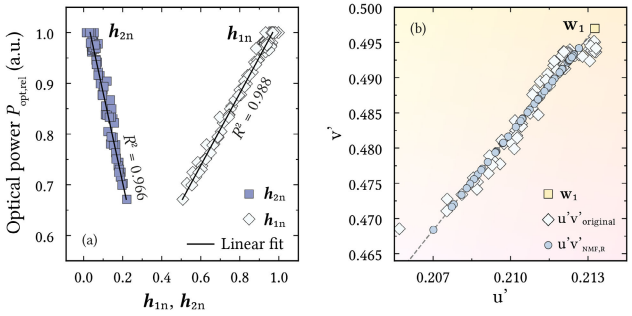

FIGURE 7. (a) Relative radiant flux depreciation vs. NMF weights h_{1n} and h_{2n} with linear curve fitting. (b) CIE 1976 UCS with original chromaticity coordinates and chromaticity coordinates from NMF + regression reconstructed spectra.

The chromaticity coordinates of the regression-based reconstructed spectra are following the trend of the base spectra's linear combination, shown in Fig. 7 (b). Given the observed linear relationship between the factorization weights and the relative radiant flux depreciation, the data were modeled using simple linear regression.

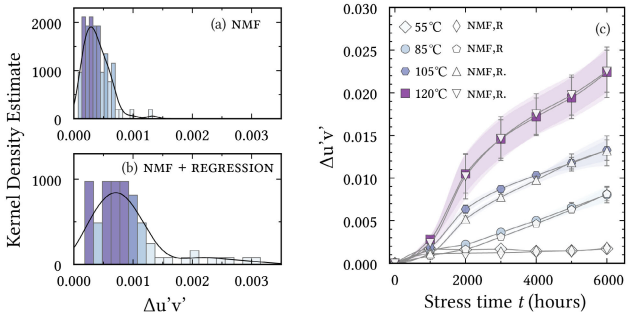

FIGURE 8. (a) Histogram of Euclidean chromaticity difference $\Delta u'v'$ between original data and spectra reconstructed by NMF. (b) Spectra reconstructed by NMF with regression. (c) Euclidean chromaticity difference for 6000 hours of stress for original data and reconstructed spectra using NMF and regression.

The uncertainties associated with this regression-based modeling are reflected in the histograms shown in Fig. 8 (a+b). By using the NMF approximation of the original spectra without regression an average chromaticity difference of $\Delta u'v'_{\mathrm{NMF}} = 0.0004$ is achieved. Modeling the determined weights (h_{1n}, h_{2n}) in dependence of relative radiant flux increases the chromaticity differences to an average of $\Delta u'v'_{\mathrm{NMF,reg}} = 0.0007$ and a predominant distribution of differences below $\Delta u'v'_{\mathrm{NMF,reg}} < 0.0015$. Subsequently, this type of reconstruction is applied to the time series of every individually measured LED. The results of the averaged chromaticity shifts per aging condition as a function of stress time are shown in Fig. 8 (c). A direct comparison with the original color shifts manifests the potential of the NMF-based modeling approach for the considered stress test period and possible extrapolations.

C. SUPERPOSITION OF PROBABILITY DENSITY FUNCTIONS

Analogously to the previous section, a number of superimposed probability functions were determined to achieve chromaticity deviations between the approximations and the original spectra smaller than $\Delta u'v'_{\mathrm{PDF}} < 0.001$. By iteratively increasing the number of PDFs, the defined chromaticity distance criterion was achieved by superimposing four Gaussian probability density functions, which are shown in Fig. 9 (a).

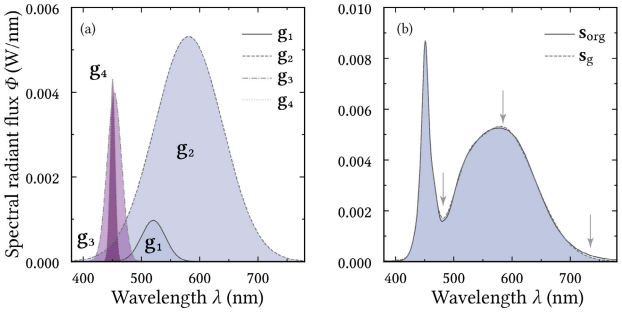

FIGURE 9. (a) Determined Gaussian distributions g_1,g_2,g_3 and g_4 for the approximation of the measured spectrum s_{org} in (b). (b) Superposition of the Gaussian distributions s_g in direct comparison with the approximated spectrum s_{org}. The areas of particularly high spectral deviations are marked with arrows.

Representatively, the spectral approximation by the superimposed Gaussian PDFs is shown in Figure 9 (b), resulting in a chromaticity difference of $\Delta u'v'_{\mathrm{PDF}} = 0.0004$. Areas of significant spectral differences between the measured spectrum and the superpositioned Gaussians are highlighted by arrows.

Subsequently, the spectral approximation is performed for all 112 measured spectra. In alignment with the procedure for the non-negative matrix factorization, the resulting fit parameters of the four Gaussian distributions are correlated with the relative radiant flux values according to Fig. 10. Linear regressions are used to estimate the parameters of

the four Gaussian distributions as a function of the relative radiant flux, thus allowing the spectra to be reconstructed for different stress times and conditions.

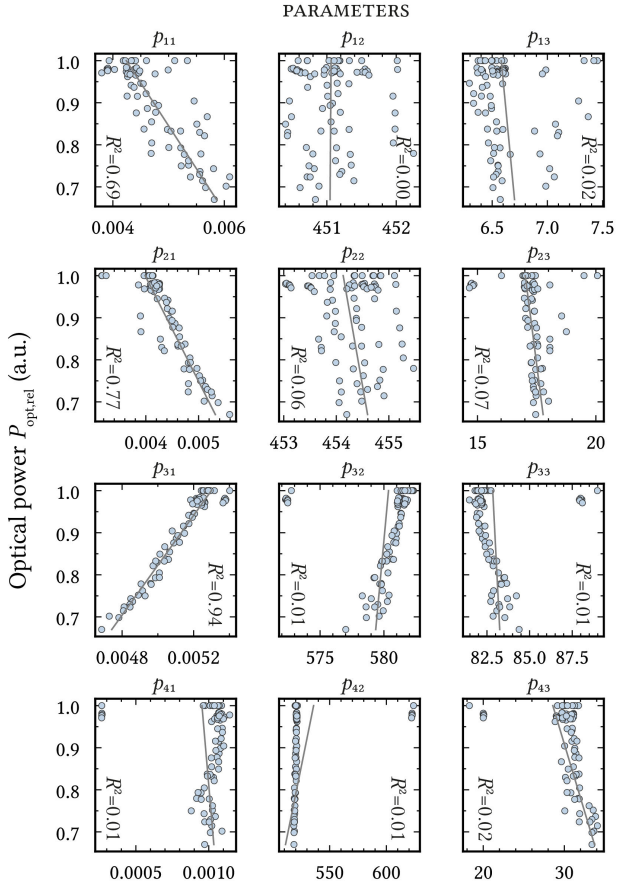

FIGURE 10. Extracted parameters p_{x1}, p_{x2} and p_{x3} of the Gaussian probability density functions g_1, g_2, g_3 and g_4 correlated with the relative radiant flux $P_{opt,rel}$.

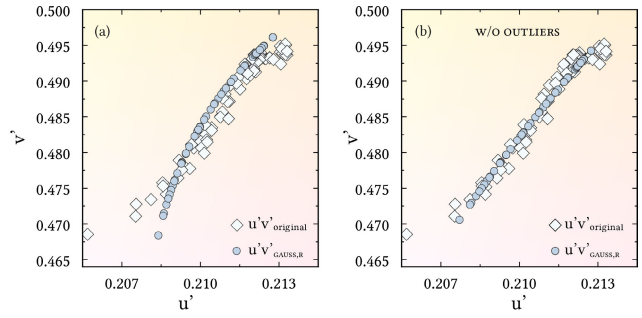

FIGURE 11. (a) CIE 1976 UCS with original chromaticity coordinates and chromaticity coordinates reconstructed from the PDFs with regressions. (b) CIE 1976 UCS with original chromaticity coordinates and chromaticity coordinates reconstructed from the PDFs using the regressions without outliers from Fig. 10.

Using this reconstruction approach, in combination with the values of the relative optical power of the measured 112 original spectra, the chromaticity coordinates result according to Figure 11 (a). In direct comparison to the coordinates of the original spectra, a systematic deviation of the chromaticity shifts with progressing stress time is observed. This model mismatch is due to the inadequate fitting of the individual regression lines shown in Figure 10, which are significantly affected by the existing outliers.

The Euclidean chromaticity distances resulting from the direct approximation of each spectrum of the 112 measured spectra are shown in the histogram in Fig. 12 (a). The mean chromaticity difference in this case is quantified with $\Delta u'v'_{\mathrm{PDF}} = 0.0005$, whereas the average difference in radiant flux can be quantified with $\Delta P_{\mathrm{opt,rel}} = 0.32\,\%$. The subsequent modeling of the parameters as a function of the relative optical power degrades the reconstruction accuracy of the spectra according to Figure 12 (b). Due to the model mismatches caused by the regressions shown in Figure 10, the mean color deviation deteriorates to $\Delta u'v'_{\mathrm{PDF,reg}} = 0.0014$.

As a result of the outlier-related mismatches, significant deviations in the chromaticity coordinates occur with increasing aging time. As a result, the color shifts of the original measurement data shown in Figure 12 (c) differ from the values of the reconstructed spectra with increasing aging time. Consequently, it can be assumed that the error in subsequent color shift extrapolations will also increase. Omitting the outliers shown in Figure 10, the quality of the model fit improves according to Fig. 11 (b). In this case, the mean chromaticity error is reduced to $\Delta u'v'_{\mathrm{PDF,reg,w/o\,outliers}} = 0.0011$ and the approximation of the temporal color shift trend becomes comparable to the results of the non-negative matrix factorization.

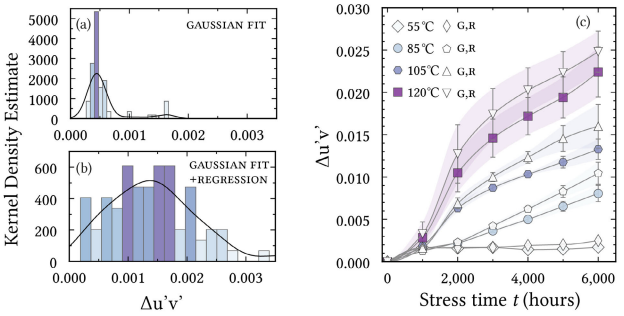

FIGURE 12. (a) Histogram of Euclidean chromaticity difference $\Delta u'v'$ between original data and spectra reconstructed by PDF. (b) Spectra reconstructed by PDF with regression. (c) Euclidean chromaticity difference for 6000 hours of stress for original data and reconstructed spectra from PDF with regression.

IV. DISCUSSION

Based on the results of the different modeling approaches, it can be stated that both approaches can be used for the spectral modeling of the analyzed data set. Both methods achieve visually imperceptible color differences of $\Delta u'v' < 0.001$ and differences in radiant flux of $\Delta P_{\mathrm{opt,rel}} \leq 0.32\,\%$ for the direct approximations of the measured spectra. Due to the linear correlation between aging-induced color shifts and radiant

flux depreciation, the two approaches show predominantly linear correlations between the model parameters and the relative radiant flux degradation. Consequently, the spectral models can be linked to the Arrhenius equation based model of temperature-induced degradation acceleration. Therefore, the combined model can be used to predict the spectra for different aging times and aging temperatures between $T_c = 55\,°C$ and $120\,°C$.

The advantages of the non-negative matrix factorization emerge primarily from the comparatively low complexity of the implementation, precise spectral approximation and a higher robustness against outliers. The robustness of the NMF against outliers is achieved by uniformly minimizing the divergence between the observation matrix $\boldsymbol{X}$ and the approximation $\boldsymbol{WH}$ using the Frobenius norm. The uniform optimization of the approximation to the observation matrix reduces the impact of slightly deviating spectra. Spectral fitting using PDF, on the other hand, is performed independently of the entire spectral data set, which means that the parameters of the individual solutions are determined independently of the overall solutions. Consequently, deviating Gaussian distribution parameters, which can be identified as outliers in Figure 10, can have a stronger impact on the subsequent modeling. This could be mitigated by a weighted regression, robust regression approaches, statistical approaches to exclude outliers or the manual exclusion of outliers.

The higher quality of the spectral approximation by the NMF results from the possibility of arbitrary continuous base spectra. While the emission spectrum of quasi-monochromatic LEDs can be described by a superposition of one or two distribution functions, the complexity of the overall spectrum increases through the use of additional phosphors. In this way, depending on the design of the phosphor mixture, a large number of local maxima can arise in the spectrum, each of which requires one or more additional distribution functions in order to be modeled appropriately. The spectral complexity of the data set used in this publication is comparatively low, even though it is representative for white LEDs. However, if more complex spectra are to be modeled, such as those of warm white LEDs using red line-emitting $Rb_5Nb_3OF_{18}:Mn^{4+}$ or $K_2SiF_6:Mn^{4+}$ phosphors [40], [41], a two-digit number of required probability distribution functions can be assumed and therefore an optimization and modeling of more than 30 parameters. If the more promising Pearson Type VII distribution function is used instead of the Gaussian functions [39], the number of parameters increases to over 60, which significantly increases the complexity of the approach.

In contrast to the superposition of probability density functions, complex spectral characteristics do not necessarily require a higher number of spectral components in the NMF approach, especially since the spectral characteristics can be represented by a few, if not just one, basis vector. This fact underlines the manageable complexity of spectral modeling using NMF. Due to the continuity criterion of the determined NMF weights on optimization level, there are gradual changes in the extracted parameters, which prove to be advantageous for modeling approaches or extrapolations of the same.

Based on additional experiments, which were not presented here, we could state that the NMF is also suitable for linear color shifts of quasi-monochromatic LEDs during lifetime, e.g. green LEDs [22], but also a variety of spectra of mono- and polychromatic LEDs, indicating c-shaped shifts in CIE 1976 UCS [46]. Consequently, the steady-state spectrum as a function of temperature and current, shifting non-linear in CIE 1976 UCS, can also be modeled by using NMF combined with multivariate regressions. In this case, the modeling requires at least 3 base vectors to span a Gamut covering the two-dimensional chromaticity shift. The weight-parameter correlation is analogous to the previous example and could be of linear or non-linear nature.

However, a limitation of the standard NMF approach arises when the factorization fails to yield smooth or physically interpretable correlations between the weight parameters and external variables such as temperature, current, or aging time. This issue can be mitigated by initializing the base vectors with Gaussian-shaped spectral functions selected to span a gamut in the CIE 1976 UCS that includes all relevant chromaticity coordinates. This increases the likelihood of obtaining a stable and physically meaningful mapping between the weight parameters and the underlying physical variables. Furthermore, the direct physical interpretability of the NMF base spectra is limited. Since the basis spectra in NMF are mathematically unconstrained, they may represent arbitrary combinations of spectral features and do not necessarily correspond to the emission spectra of individual LEDs or phosphor materials. Nonetheless, the resulting base spectra often reflect significant changes in the overall spectral distribution and can capture relevant spectral dynamics that are critical for chromaticity and colorimetric analysis.

As a result, the proposed spectral modeling approach using non-negative matrix factorization performs on par with state-of-the-art methods and offers clear advantages in terms of accuracy and robustness. A detailed comparison of the proposed approach and the state-of-the-art method based on various evaluation criteria is provided in Table 2. A computational time comparison was not included, as the spectral models are typically created offline on standard computing systems. After this initial model generation, both approaches result in models that are computationally efficient and simple enough to be deployed in real-time or embedded systems without significant performance constraints.

Due to the gradual nature of extracted NMF weights, it is promising for the spectral model in multi-domain model based digital twins of light-emitting diodes [47]. Output or input parameters of the multi-domain models, such as optical power, case temperature, or forward current, could be directly linked to the spectral model. To improve the concept of spectral LED modeling using NMF, we envision future

research to determine reproducible and dataset-independent solutions for basis vectors and weights spanning a gamut that covers the relevant color coordinates while exhibiting correlations to the physical parameters under consideration. Although giving spectra or weights as initial guesses proves to be target-oriented, since a different weighting of the observation matrix spectra based on its calculated chromaticity coordinates increases the accuracy of the spectral model even further.

TABLE 2. Comparison of PDF and NMF for spectral modeling.

Criterion	PDF fitting	NMF
Interpretability	**High** Each function predefined and often physically meaningful	**Medium** Basis vectors learned from data, less intuitive
Flexibility	**Low** Limited by chosen function type (e.g., Gaussian)	**High** Arbitrary spectral forms can be captured
Outlier Robustness	**Low** Each spectrum fitted separately, sensitive to deviations	**High** Global optimization reduces sensitivity to single-spectrum outliers
Model complexity	**High** Many parameters required for complex spectra	**Low** Few components are often sufficient for accurate modeling
Extrapolation	**Medium** Parameter trends must be modeled separately	**High** Smooth weight variation enables direct extrapolation

V. CONCLUSION

In summary, we report on two spectral degradation models of light-emitting diodes, which are capable of modeling the spectral characteristics for different stress test temperatures and an operation period of 6000 hours. The state of the art probability density function model is evaluated against an unsupervised machine learning approach based on non-negative matrix factorization. With respect to the spectral reconstruction accuracy, the NMF approach is outperforming the superposition of Gaussian probability density functions. Due to temperature accelerated degradation of the devices, the radiant flux depreciation for temperatures between $T_c = 55\,°C$ and $T_c = 120\,°C$ can be modeled using the Arrhenius equation. The linear correlation between the relative radiant flux values and the extracted NMF parameters, allows a subsequent reconstruction of spectra for different operating temperatures between $T_c = 55\,°C$ and $T_c = 120\,°C$ and aging times between 0 hours and 6000 hours. Consequently, a different modeling approach was introduced, allowing to predict the temperature-dependent spectral characteristics over the aging period of the analyzed data set with a reconstruction accuracy primarily below $\Delta u'v' < 0.001$. To further evaluate the modeling capabilities of the approach, spectral temperature and current dependencies, combined with spectral degradation dynamics, will be analyzed using additional data sets in subsequent publications. The implementation of the proposed approach and the dataset are available at https://github.com/LightingSystemLab, allowing other researchers to use, reproduce, and validate the presented results.

ACKNOWLEDGMENT

The work reported in this article reflects the author's view and that the JU is not responsible for any use that may be made of the information it contains.

REFERENCES

[1] G. Bobashev, N. G. Baldasaro, K. C. Mills, and J. L. Davis, "An efficiency-decay model for lumen maintenance," *IEEE Trans. Device Mater. Rel.*, vol. 16, no. 3, pp. 277–281, Sep. 2016, doi: 10.1109/TDMR.2016.2584926.

[2] W. D. van Driel, M. Schuld, B. Jacobs, F. Commissaris, J. van der Eyden, and B. Hamon, "Lumen maintenance predictions for LED packages," *Microelectron. Rel.*, vol. 62, pp. 39–44, Jul. 2016, doi: 10.1016/j.microrel.2016.03.018.

[3] M. S. Ibrahim, J. Fan, W. K. C. Yung, Z. Wu, and B. Sun, "Lumen degradation lifetime prediction for high-power white LEDs based on the gamma process model," *IEEE Photon. J.*, vol. 11, no. 6, pp. 1–16, Dec. 2019, doi: 10.1109/JPHOT.2019.2950472.

[4] M. Buffolo, A. Caria, F. Piva, N. Roccato, C. Casu, C. De Santi, N. Trivellin, G. Meneghesso, E. Zanoni, and M. Meneghini, "Defects and reliability of GaN-based LEDs: Review and perspectives," *Phys. Status Solidi (A)*, vol. 219, no. 8, Apr. 2022, Art. no. 2100727, doi: 10.1002/pssa.202100727.

[5] *Projecting Long-Term Lumen, Photon, and Radiant Flux Maintenance of LED Light Sources*, Standard IES TM-21–19, Illuminating Engineering Society, 2019.

[6] N. Santhi, H. C. Thorne, D. R. van der Veen, S. Johnsen, S. L. Mills, V. Hommes, L. J. M. Schlangen, S. N. Archer, and D.-J. Dijk, "The spectral composition of evening light and individual differences in the suppression of melatonin and delay of sleep in humans," *J. Pineal Res.*, vol. 53, no. 1, pp. 47–59, Aug. 2012, doi: 10.1111/j.1600-079x.2011.00970.x.

[7] L. Schlangen, S. Belgers, R. Cuijpers, B. Zandi, and I. Heynderickx, "Correspondence: Designing and specifying light for melatonin suppression, non-visual responses and integrative lighting solutions–establishing a proper bright day, dim night metrology," *Lighting Res. Technol.*, vol. 54, no. 8, pp. 761–777, Dec. 2022.

[8] J. A. Enezi, V. Revell, T. Brown, J. Wynne, L. Schlangen, and R. Lucas, "A 'Melanopi' spectral efficiency function predicts the sensitivity of melanopsin photoreceptors to polychromatic lights," *J. Biol. Rhythms*, vol. 26, no. 4, pp. 314–323, Aug. 2011, doi: 10.1177/0748730411409719.

[9] B. Zandi, O. Stefani, A. Herzog, L. J. M. Schlangen, Q. V. Trinh, and T. Q. Khanh, "Optimising metameric spectra for integrative lighting to modulate the circadian system without affecting visual appearance," *Sci. Rep.*, vol. 11, no. 1, p. 23188, Nov. 2021.

[10] V. L. Revell, D. C. G. Barrett, L. J. M. Schlangen, and D. J. Skene, "Predicting human nocturnal nonvisual responses to monochromatic and polychromatic light with a melanopsin photosensitivity function," *Chronobiology Int.*, vol. 27, no. 9, pp. 1762–1777, Dec. 2010, doi: 10.3109/07420528.2010.516048.

[11] M. C. Giménez, O. Stefani, C. Cajochen, D. Lang, G. Deuring, and L. J. M. Schlangen, "Predicting melatonin suppression by light in humans: Unifying photoreceptor-based equivalent daylight illuminances, spectral composition, timing and duration of light exposure," *J. Pineal Res.*, vol. 72, no. 2, p. 12786, Mar. 2022, doi: 10.1111/jpi.12786.

[12] F. Reifegerste and J. Lienig, "Modelling of the temperature and current dependence of LED spectra," *J. Light Vis. Environ.*, vol. 32, no. 3, pp. 288–294, 2008, doi: 10.2150/jlve.32.288.

[13] A. Vaskuri, H. Baumgartner, P. Kärhä, G. Andor, and E. Ikonen, "Modeling the spectral shape of InGaAlP-based red light-emitting diodes," *J. Appl. Phys.*, vol. 118, no. 20, Nov. 2015, Art. no. 203103, doi: 10.1063/1.4936322.

[14] A. Vaskuri, P. Kärhä, H. Baumgartner, O. Kantamaa, T. Pulli, T. Poikonen, and E. Ikonen, "Relationships between junction temperature, electroluminescence spectrum and ageing of light-emitting diodes," *Metrologia*, vol. 55, no. 2, pp. S86–S95, Apr. 2018, doi: 10.1088/1681-7575/aaaed2.
[15] A. Keppens, W. R. Ryckaert, G. Deconinck, and P. Hanselaer, "Modeling high power light-emitting diode spectra and their variation with junction temperature," *J. Appl. Phys.*, vol. 108, no. 4, Aug. 2010, Art. no. 043104, doi: 10.1063/1.3463411.
[16] J. Huang, D. S. Golubovic, S. Koh, D. Yang, X. Li, X. Fan, and G. Q. Zhang, "Degradation mechanisms of mid-power white-light LEDs under high-temperature–humidity conditions," *IEEE Trans. Device Mater. Rel.*, vol. 15, no. 2, pp. 220–228, Jun. 2015.
[17] M. Dal Lago, M. Meneghini, N. Trivellin, G. Meneghesso, and E. Zanoni, "Degradation mechanisms of high-power white LEDs activated by current and temperature," *Microelectron. Rel.*, vol. 51, nos. 9–11, pp. 1742–1746, Sep. 2011.
[18] G. Meneghesso, M. Meneghini, and E. Zanoni, "Recent results on the degradation of white LEDs for lighting," *J. Phys. D, Appl. Phys.*, vol. 43, no. 35, Sep. 2010, Art. no. 354007.
[19] M. Wagner, A. Herzog, H. Ganev, and T. Khanh, "Lifetime calculation of white hp-leds from 16,000 hours aging data," *LED Prof. Rev.*, vol. 59, pp. 34–38, 2017.
[20] M. Wagner, A. Herzog, H. Ganev, and T. Q. Khanh, "LED aging acceleration—An analysis from measuring and aging data of 14,000 hours LED degradation," in *Proc. 12th China Int. Forum Solid State Lighting (SSLCHINA)*, China, Nov. 2015, pp. 75–78.
[21] E. Jung and H. Kim, "Rapid optical degradation of GaN-based light-emitting diodes by a current-crowding-induced self-accelerating thermal process," *IEEE Trans. Electron Devices*, vol. 61, no. 3, pp. 825–830, Mar. 2014.
[22] A. Herzog, M. Wagner, and T. Q. Khanh, "Efficiency droop in green InGaN/GaN light emitting diodes: Degradation mechanisms and initial characteristics," *Microelectron. Rel.*, vol. 112, Sep. 2020, Art. no. 113792, doi: 10.1016/j.microrel.2020.113792.
[23] T. K. Law and F. Lim, "A practical degradation based method to predict long-term moisture incursion and color change in high power LEDs," *IEEE Photon. J.*, vol. 10, no. 5, pp. 1–14, Oct. 2018.
[24] A. Herzog, M. Wagner, and T. Q. Khanh, "Monitoring the optical degradation of green light-emitting diodes on the basis of measured electrical characteristics," *Microelectron. Rel.*, vol. 121, Jun. 2021, Art. no. 114147.
[25] B.-M. Song and B. Han, "Spectral power distribution deconvolution scheme for phosphor-converted white light-emitting diode using multiple Gaussian functions," *Appl. Opt.*, vol. 52, no. 5, pp. 1016–1024, 2013, doi: 10.1364/ao.52.001016.
[26] Z. Guo, T. Shih, Y. Gao, Y. Lu, L. Zhu, G. Chen, Y. Lin, J. Zhang, and Z. Chen, "Optimization studies of two-phosphor-coated white light-emitting diodes," *IEEE Photon. J.*, vol. 5, no. 2, Apr. 2013, Art. no. 8200112, doi: 10.1109/JPHOT.2013.2245885.
[27] R. Supronowicz and I. Fryc, "The LED spectral power distribution modelled by different functions–how spectral matching quality affected computed LED color parameters," in *Proc. 2nd Balkan Junior Conf. Lighting (Balkan Light Junior)*, Sep. 2019, pp. 1–4, doi: 10.1109/BLJ.2019.8883564.
[28] M. E. Raypah, M. Devarajan, and F. Sulaiman, "Modeling spectra of low-power SMD LEDs as a function of ambient temperature," *IEEE Trans. Electron Devices*, vol. 64, no. 3, pp. 1180–1186, Mar. 2017, doi: 10.1109/TED.2017.2656862.
[29] D. Mozyrska and I. Fryc, "Approximation of spectroradiometric data by fractional model," *Przeglad Elektrotechniczny*, vol. 87, no. 2, pp. 255–257, 2011.
[30] W. Chen, J. Fan, C. Qian, B. Pu, X. Fan, and G. Zhang, "Reliability assessment of light-emitting diode packages with both luminous flux response surface model and spectral power distribution method," *IEEE Access*, vol. 7, pp. 68495–68502, 2019, doi: 10.1109/ACCESS.2019.2916878.
[31] H. Chen and S. Y. Hui, "Dynamic prediction of correlated color temperature and color rendering index of phosphor-coated white light-emitting diodes," *IEEE Trans. Ind. Electron.*, vol. 61, no. 2, pp. 784–797, Feb. 2014, doi: 10.1109/TIE.2013.2251736.
[32] J. Fan, M. G. Mohamed, C. Qian, X. Fan, G. Zhang, and M. Pecht, "Color shift failure prediction for phosphor-converted white LEDs by modeling features of spectral power distribution with a nonlinear filter approach," *Materials*, vol. 10, no. 7, p. 819, Jul. 2017, doi: 10.3390/ma10070819.
[33] J. Fan, W. Chen, W. Yuan, X. Fan, and G. Zhang, "Dynamic prediction of optical and chromatic performances for a light-emitting diode array based on a thermal-electrical-spectral model," *Opt. Exp.*, vol. 28, no. 9, pp. 13921–13937, 2020, doi: 10.1364/oe.387660.
[34] J. Fan, Y. Li, I. Fryc, C. Qian, X. Fan, and G. Zhang, "Machine-learning assisted prediction of spectral power distribution for full-spectrum white light-emitting diode," *IEEE Photon. J.*, vol. 12, no. 1, pp. 1–18, Feb. 2020, doi: 10.1109/JPHOT.2019.2962818.
[35] C. Qian, J. Fan, X. Fan, and G. Zhang, "Prediction of lumen depreciation and color shift for phosphor-converted white light-emitting diodes based on a spectral power distribution analysis method," *IEEE Access*, vol. 5, pp. 24054–24061, 2017, doi: 10.1109/ACCESS.2017.2716354.
[36] U. J. Blaszczak and L. Gryko, "High-quality multi-emitter LED-based retrofits for incandescent photometric a illuminant reliability of R2 evaluation," *Appl. Sci.*, vol. 14, no. 13, p. 5717, Jun. 2024. [Online]. Available: https://www.mdpi.com/2076-3417/14/13/5717
[37] J. Lokesh, A. Padmasali, M. Mahesha, and S. G. Kini, "An analytical and machine learning model for SPD estimation and its prediction for lumen and chromaticity shift based LED lifetime performance analysis," *Phys. Scripta*, vol. 99, no. 7, Jul. 2024, Art. no. 076018.
[38] J. Lokesh, S. G. Kini, M. G. Mahesha, and A. N. Padmasali, "Color-based lifetime estimation of LEDs using spectral power distribution prediction through analytical and machine learning models," *IEEE Access*, vol. 13, pp. 61665–61674, 2025.
[39] S. Benkner, A. Herzog, S. Klir, W. D. Van Driel, and T. Q. Khanh, "Advancements in spectral power distribution modeling of light-emitting diodes," *IEEE Access*, vol. 10, pp. 83612–83619, 2022, doi: 10.1109/ACCESS.2022.3197280.
[40] Z. Yang, Z. Yang, Q. Wei, Q. Zhou, and Z. Wang, "Luminescence of red-emitting phosphor Rb5Nb3OF18: Mn4+ for warm white light-emitting diodes," *J. Lumin.*, vol. 210, pp. 408–412, Jun. 2019. [Online]. Available: https://www.sciencedirect.com/science/article/pii/S0022231318317435
[41] S. Hariyani, J. Brgoch, F. Garcia-Santamaria, S. P. Sista, J. E. Murphy, and A. A. Setlur, "From lab to lamp: Understanding downconverter degradation in LED packages," *J. Appl. Phys.*, vol. 132, no. 19, Nov. 2022, Art. no. 190901.
[42] A. Herzog, M. Wagner, S. Benkner, B. Zandi, W. D. van Driel, and T. Q. Khanh, "Long-term temperature-dependent degradation of 175 w chip-on-board LED modules," *IEEE Trans. Electron Devices*, vol. 69, no. 12, pp. 6830–6836, Dec. 2022, doi: 10.1109/TED.2022.3214169.
[43] R. Hamamoto, K. Takasawa, H. Machino, K. Kobayashi, S. Takahashi, A. Bolatkan, N. Shinkai, A. Sakai, R. Aoyama, M. Yamada, K. Asada, M. Komatsu, K. Okamoto, H. Kameoka, and S. Kaneko, "Application of non-negative matrix factorization in oncology: One approach for establishing precision medicine," *Briefings Bioinf.*, vol. 23, no. 4, p. 246, Jul. 2022, doi: 10.1093/bib/bbac246.
[44] G. Chennupati, R. Vangara, E. Skau, H. Djidjev, and B. Alexandrov, "Distributed non-negative matrix factorization with determination of the number of latent features," *J. Supercomput.*, vol. 76, no. 9, pp. 7458–7488, Sep. 2020, doi: 10.1007/s11227-020-03181-6.
[45] The Scikit-Learn Developers, "Scikit-learn," Zenodo, Version 1.7.1, CERN, Geneva, Switzerland, Jul. 2025, doi: 10.5281/zenodo.16086009.
[46] M. Cai, D. Yang, J. Huang, M. Zhang, X. Chen, C. Liang, S. Koh, and G. Zhang, "Color shift modeling of light-emitting diode lamps in step-loaded stress testing," *IEEE Photon. J.*, vol. 9, no. 1, pp. 1–14, Feb. 2017, doi: 10.1109/JPHOT.2016.2634702.
[47] A. Poppe, G. Farkas, L. Gaál, G. Hantos, J. Hegedüs, and M. Rencz, "Multi-domain modelling of LEDs for supporting virtual prototyping of luminaires," *Energies*, vol. 12, no. 10, p. 1909, May 2019, doi: 10.3390/en12101909.

ALEXANDER HERZOG (Senior Member, IEEE) received the B.Sc., M.Sc., and Ph.D. degrees in electrical engineering from the Technische Universität Darmstadt, in 2012, 2015, and 2020, respectively. Currently, he is a Postdoctoral Researcher and a Research Group Leader with the Laboratory of Adaptive Lighting Systems and Visual Processing, Technische Universität Darmstadt. His research interests include lifetime prediction, reliability analysis, and digital twins of light-emitting diodes. Additional research topics are temporal light artifacts and visual neuro-stimulation.

BENOIT HAMON was born in France, in 1988. He received the Engineering degree in material sciences and nanotechnologies and the Ph.D. degree in LED reliability, in 2011 and 2014, respectively. Then, he joined the industry leader Signify, as an LED Expert concentrating on LED modeling and reliability. In 2018, he joined Pi Lighting, as a Senior Scientist using his expertise for various players of the lighting industry.

PAUL MYLAND received the B.Sc. and M.S. degrees in electrical engineering and information technology from the Technical University of Darmstadt, Germany, in 2016 and 2019, respectively, and the Ph.D. degree from the Laboratory of Adaptive Lighting Systems and Visual Processing, in 2024. Since then, he has been a Research Assistant with the Laboratory of Adaptive Lighting Systems and Visual Processing. His current work focuses on applications of spectral sensors and miniature spectrometers in lighting control. His broader research interests include color and lighting quality, color perception, museum lighting, and multidimensional lighting optimization.

PETER FOERSTER (Senior Member, IEEE) received the B.Sc. and M.Sc. degrees in electrical engineering from the Technical University of Darmstadt. Currently, he is a Doctoral Researcher with the Computational Electromagnetics Group, Technical University of Darmstadt, and the Centre for Analysis, Scientific Computing and Applications, Eindhoven University of Technology. His research interests include circuit simulation, differential-algebraic equations, digital twins, and machine learning.

SIMON BENKNER received the B.Sc., M.Sc., and Ph.D. degrees in electrical engineering from the Technical University of Darmstadt, Germany, in 2015, 2017, and 2023, respectively. Currently, he is active as an Academic Lecturer and also works as a Developer and a Consultant for electronic circuits. His research interests primarily focus on the reliability of electronic systems, with particular emphasis on LED technologies and degradation modeling. Additionally, his work explores advancements in smart electronics and the Internet of Things (IoT).

BABAK ZANDI received the M.Sc. and Ph.D. degrees in electrical engineering and information technology from the Technical University of Darmstadt. He was a Research Group Leader with the Laboratory of Adaptive Lighting Systems and Visual Processing, Darmstadt. Currently, he is an AI Expert in the banking sector with a focus on transformer-based large language models and a Lecturer with the Technical University of Darmstadt. His scientific interests include the integration of neural networks in heuristic optimization algorithms and the modeling of time-series data. He served as an Editorial Board Member for *Scientific Reports*.

VICTOR GUERRA received the degree in telecommunication engineering and the Ph.D. degree in cybernetics and telecommunication from the Universidad de Las Palmas de Gran Canaria (ULPGC). He boasts an extensive track record spanning over a decade in the field of photonics technology and communications. His professional experience comprises an array of projects, including four H2020 initiatives and other collaborative research efforts. He has also authored over 75 scientific publications encompassing a range of formats. His work traverses optical wireless communication, optical camera communication, and the Internet of Things and their intersection with deep learning.

SEBASTIAN SCHOEPS (Senior Member, IEEE) received the M.Sc. degree in business mathematics from the Bergische Universität Wuppertal and the joint Ph.D. degree in mathematics and physics from the Katholieke Universiteit Leuven. In 2012, he was appointed as a Professor of computational electromagnetics with the Interdisciplinary Centre of Computational Engineering and the Department of Electrical Engineering and Information Technology, Technische Universität Darmstadt. His current research interests include coupled multiphysical problems, bridging computer-aided design and simulation, parallel algorithms for high performance computing, digital twins, uncertainty quantification, and machine learning.

WILLEM D. VAN DRIEL received the degree in mechanical engineering from the Technical University of Eindhoven and the Ph.D. degree from Delft University of Technology, The Netherlands. He has more than 25 year track record in the reliability domain, application areas range from healthcare, gas and oil explorations, and semiconductors. His current position is a Fellow Scientist with Signify (formerly Philips Lighting). Besides that, he holds a professor position with the University of Delft, The Netherlands. He has authored or co-authored more than 350 scientific publications, including journal and conference papers, book or book chapters, and invited keynote lectures. His scientific interests include solid state lighting, microelectronics and microsystems technologies, virtual prototyping, virtual reliability qualification, and designing for reliability of microelectronics and microsystems. He is the Chair of the organizing committee of the IEEE Conference EuroSimE.

TRAN QUOC KHANH received the Dr.-Ing. degree in physics and technology of electronic components and the Habilitation degree in mechanical engineering and technical optics from the Institute for Lighting Technology, Technische Universität Ilmenau, Germany, in 1989 and 2005, respectively. Since 2006, he has been a Full Professor and the Head of the Laboratory of Adaptive Lighting Systems and Visual Processing, Technical University of Darmstadt, where he has been the Dean of the Department of Electrical Engineering and Information Technology, since 2018. He leads research groups in the field of automotive lighting, human-centric lighting, smart indoor lighting, and LED technology.